J Mol Model (2017) 23:214
DOI 10.1007/s00894-017-3385-x

ORIGINAL PAPER

Effects of varying the 6-position oxidation state of hexopyranoses: a systematic comparative computational analysis of 48 monosaccharide stereoisomers

Alison E. Vickman[1] · Daniel C. Ashley[1] · Mu-Hyun Baik[1,2,3] · Nicola L. B. Pohl[1]

Received: 23 February 2017 / Accepted: 4 June 2017

Abstract Knowledge of multi-dimensional carbohydrate structure is essential when delineating structure–function relationships in the development of analytical techniques such as ion mobility-mass spectrometry and of carbohydrate-based therapeutics, as well as in rationally modifying the chemical and physical properties of drugs and materials based on sugars. Although monosaccharides are conventionally presumed to adopt the canonical $^4C_1$ chair conformation, it is not well known how altering the substituent identity around the pyranose ring affects the favored conformational state. This work provides a comprehensive and systematic computational comparison of all eight aldohexose isomers in the gas phase with reduction and oxidation at the C-6 position using density functional theory (M05-2X/cc-pVTZ(−f)//B3LYP/6-31G**) to determine the conformational and anomeric preference for each sugar in the gas phase. All 6-deoxyhexose and aldohexose isomers favored the $^4C_1$ chair conformation, while oxidation at C-6 showed a shift in equilibrium to favor the $^1C_4$ chair for β-alluronic acid, β-guluronic acid, and β-iduronic acid. The anomeric preference was found to be significantly affected by a remote change in oxidation state, with the alternate anomer favored for several isomers. These findings provide a fundamental platform to empirically test steric and electronic effects of pyranose substituents, with the goal of formulating straightforward rules that govern carbohydrate reactivity and drive quicker, more efficient syntheses.

Keywords Carbohydrates · Conformational analysis · Density functional theory

Electronic supplementary material The online version of this article (doi:10.1007/s00894-017-3385-x) contains supplementary material, which is available to authorized users.

✉ Mu-Hyun Baik
mbaik2805@kaist.ac.kr

✉ Nicola L. B. Pohl
npohl@indiana.edu

[1] Department of Chemistry, Indiana University, Bloomington, IN 47405, USA

[2] Department of Chemistry, Korea Advanced Institute of Science and Technology (KAIST), Daejeon 34141, South Korea

[3] Center for Catalytic Hydrocarbon Functionalizations, Institute for Basic Science (IBS), Daejeon 34141, South Korea

Introduction

Understanding molecular reactivity and selectivity in both synthetic and biological systems often relies on our knowledge of physical and electronic structural features. The basis of many principles of conformational analysis, including ring conformation and stereochemistry, have benefited from the study of carbohydrate structures. Extensive investigations of these structure–reactivity relationships have provided key insights in chemical stability, prediction of reaction products, and reaction mechanism interpretation [1]. However, a detailed, comparative interrogation of the discrete conformational states of the diverse array of carbohydrates has been greatly limited by their inherent conformational heterogeneity [2]. Knowledge of the rich conformational landscapes of these highly dynamic molecules promises to catalyze more straightforward routes for carbohydrate synthesis at a time of increased interest in automating oligosaccharide synthesis [3].

The high degree of flexibility and conformational complexity associated with these molecules due to their ability to adopt several different ring conformations and a large number of low energy rotameric states makes studying their conformational landscape a challenging task. Although pyranose rings

Published online: 27 June 2017

predominantly adopt the $^4C_1$ chair conformation, the conversion to other puckered forms (skew-boat, boat, half-chair, envelope) may be energetically feasible depending on the nature and orientation of exocyclic substituents attached to the ring [1, 4]. In addition, the rotational freedom of the secondary hydroxyl groups and hydroxymethyl side-chain of a monosaccharide adds an additional degree of complexity. In principle, a total of $3^5 = 729$ rotamers can be generated for a given pyranose ring considering the three-fold rotation of each substituent bond [5]. The stereochemical configuration of the anomeric carbon, in either the alpha or beta orientation, must also be taken into account, thereby doubling the number of isomers to evaluate. In an effort to minimize the number of structures in the sugar set and limit the subsequent calculations needed, only the canonical chair ($^4C_1$ and $^1C_4$) conformations will be investigated in this study since they are commonly found to be the lowest in energy [1].

As an alternative to conventional spectroscopic methods, which are limited by conformational averaging and lack detailed structural information, computational methods can provide a theoretical understanding of the broader carbohydrate conformational landscape, and thereby more accurately probe the population of conformers present in multiple phases (i.e., gas, solution, solid-state) [6]. In this respect, computation can also illuminate specific structural features and the relative stability of conformational states can be quantitatively determined. Several studies using both molecular mechanics and quantum mechanical methods at various levels of theory have focused on determining individual monosaccharide conformations, while others have compared the energetic and conformational differences for small subsets of sugars [7–31]. Not surprisingly though, given the complexity of the calculations required, relatively few calculations have been published to date, with those few focused primarily on the small subset of mammalian sugars. A few computational studies incorporating all eight possible hexopyranose isomers of glucose monosaccharides have been published recently, and confirm a predominantly $^4C_1$ chair conformation for these structures [32, 33], but comparisons to the also common 6-deoxysugars and uronic acids are still lacking. The conformational space of the deoxyhexoses and hexuronic acids—both found in a range of natural materials such as rhamnans, pectins and hyaluronic acid—is still relatively unexplored; with very few of these sugar structures studied in depth or at all (Fig. 1) [34–39].

Other studies have quantitatively compared NMR J-couplings to density functional theory (DFT) solvation calculations to validate and refine molecular dynamics (MD) simulations and determine substituent conformation in aqueous solution [40, 41]. Although the conformational shape of these highly polarized molecules is fairly flexible in solution, and interaction with solvent molecules may cause changes in conformation [29, 42], accurately incorporating solvation effects in computer models remains a significant challenge. Polarizable continuum models (PCM), which treat the solvent implicitly, have been frequently employed for modeling solvated systems, due to their low computational cost, and often excellent predictive power. Although polarizable continuum models do work well in a number of cases, based on previous computational work on carbohydrates [43–45], it is likely that MD simulations would be required to accurately model aqueous solvation of the sugar substrates studied within this work, due primarily to the neglect of explicit hydrogen-bonding interactions and bulk solvent effects in PCM models [46]. MD simulations that promise the most sophisticated handling of solvation effects are unfortunately often time-intensive and computationally expensive. As a result, there are very few DFT-MD studies on sugars found in the literature, with typically only one structure investigated per publication due to the more intensive nature of these simulations. Solvation of sugar substrates is still not well understood and much more work in this area (using both explicit and implicit solvation models) is needed to ensure accurate representation of aqueous solvation of sugars.

With these technical and conceptual limitations in mind, we chose to limit ourselves to gas phase structures to establish a consistent baseline for future comparisons between inherent sugar conformations *in vacuo* and protected sugar derivatives, ultimately providing a reference for conformational changes due to electronic or steric factors, as well as intramolecular interactions. While neglecting solvation will certainly lead to our results being less accurate for making predictions of aqueous behavior, gas-phase calculations provide useful fundamental and practical information. In fact, most protected sugars are not actually soluble in water, but are soluble in nonpolar solvents such as dichloromethane (DCM) and toluene. Gas phase calculations may not drastically differ from results obtained using more commonly applied, low dielectric solvents. Our calculated protected sugar structures can ultimately be further validated using NMR and solvation models with the low dielectric, non-coordinating solvents commonly used in glycosylation reactions.

The present work therefore aims to elucidate the electronic and steric implications of oxidizing or reducing the hydroxymethyl substituent at the 6-position to the carboxylic acid or methyl group, respectively, in the first systematic computational study of all the possible glucose stereoisomers, as well as answer several key questions. Does this picture of predominantly $^4C_1$ chair conformations hold for all anomers of all possible glucose isomers even when the oxidation state at the exocyclic carbon changes or do some anomers prefer the alternate $^1C_4$ chair conformation? Does the anomeric effect always dictate the dominant anomeric isomer regardless of the stereochemistry of the remaining substituents? Does the oxidation state at the remote 6-position affect this anomeric ratio?

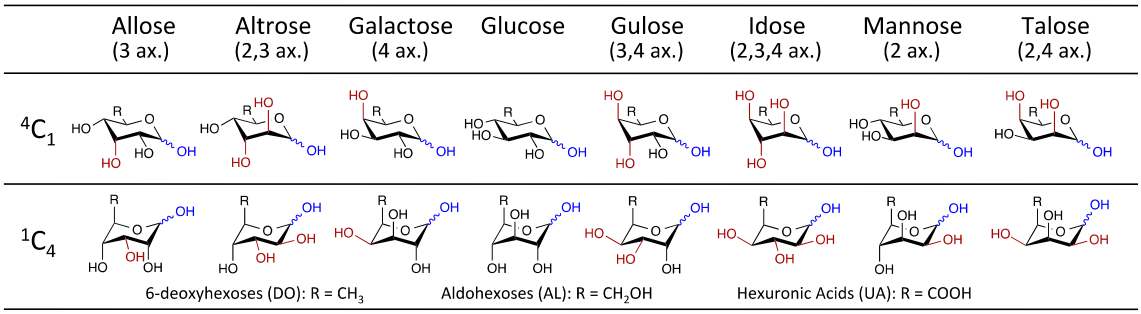

Fig. 1 The ninety-six 6-deoxyhexose, aldohexose, and hexuronic acid structures investigated

Computational methods

The conformational landscape of each stereoisomer was initially investigated by performing a Monte-Carlo type conformational search to generate a series of unique monosaccharide rotamers for a given structure using the Global-MMX program (GMMX) in PC Model 9.30 [47] employing the MMX force field which is derived from MM2 with π-VESCF routines taken from the MMP1 program [48–50]. The π-VESCF routines were modified for open shell species by McKelvey, whereas Gajewski improved the calculations of heat of formation. A large number of low energy rotamers were located, but only structures that were within 4.00–4.50 kcal mol^{-1} of the nearest low energy rotamer were included in the final set. Due to occasional unwanted relaxation of the ring geometry to skew-boat or boat-like structures during the conformational search, a substructure method was employed to freeze the ring atoms and maintain ring conformation throughout the simulation in order to avoid ring interconversion and epimerization. For all chair conformers, a substructure of the ring atoms was created and not minimized during the rotamer search.

The use of GMMX allowed a rapid generation of relevant conformers, but to get a more accurate picture of the energetics, this set of structures was additionally characterized with higher-level electronic structure calculations. Further optimization using DFT was carried out in the Jaguar 8.1 suite of ab initio quantum chemistry programs [51]. Geometry optimizations and vibrational entropies were calculated at the B3LYP/6-31G** level of theory [52], followed by additional single point calculations using the Minnesota functional M05-2X [53] and Dunning's correlation-consistent polarized triple-ζ basis set cc-pVTZ(−f), which includes a double set of polarization functions on all atoms [54]. Frequency calculations confirmed all structures were true minima. Energy components were calculated as follows:

$$\Delta G(\text{gas}) = \Delta H(\text{gas}) - T\Delta S(\text{gas}) \quad (1)$$

$$\Delta H(\text{gas}) = \Delta E(\text{SCF}) + \Delta ZPE \quad (2)$$

where ΔG(gas) is the change in gas phase free energy; ΔH(gas) is the change in gas phase enthalpy; T is temperature (298.15 K); ΔS(gas) is the change in gas phase entropy; ΔE(SCF) is the self-consistent field energy, i.e., "raw" electronic energy as calculated at the triple-ζ level using M05-2X unless noted otherwise; ΔZPE is the change in vibrational zero point energy (ZPE).

Duplicate structures present after geometry optimization were removed by carrying out a statistical analysis, wherein the root-mean-square deviation (RMSD) was calculated for all rotamer populations. Quantitative comparison of RMSD values revealed similarity in three-dimensional (3D) structure based on atomic coordinate displacement. Duplicate rotamers were subsequently removed from the data set. Anomeric ratios are calculated using relative free-energy values for the total rotamer ensemble. Monosaccharide nomenclature is available in the SI (Fig. S2).

The choice of functional for obtaining final Gibbs free energies is based on previous work showing improved accuracy for monosaccharide modeling compared to the popular B3LYP exchange-correlation functional, even with dispersion corrections added [55, 56]. A functional and basis set screen was also performed confirming M05-2X had the best agreement with MP2 calculations (Fig. S1). It is important to note that to actually distinguish between small differences in anomeric ratios (i.e., 70:30 vs. 30:70) involves accurately calculating relative energetics on the order of less than 1 kcal mol^{-1}. Generally this is considered well beyond the error limit of modern DFT as shown in several benchmarking studies [57–59]. Despite this, we are optimistic about the accuracy of the results reported herein for several reasons. Previous work by Schnupf and coworkers showed that DFT methods could be used to accurately determine anomeric ratios based on comparison with experimentally determined values [28]. We found that, despite using different methodology for our conformational searches, we obtained results similar to this work in most cases, suggesting that our computational methods likely have the same level of rigor. Exceptions to this are discussed below. We believe that the high accuracy of DFT in this case can be ascribed to the fact that we are comparing structures that are both extremely similar to each other, and in all cases relatively simple as well. This leads to massive error cancelations for our purpose of determining the

conformational landscape. It is still always dangerous to over-interpret calculated data, however, and hence we emphasize that our most important results are the qualitative trends predicted by our calculations.

Results and discussion

Lowest energy monosaccharide conformations

In order to examine the conformational differences between monosaccharides with varying oxidation states at the 6-position, the key findings concerning the lowest energy conformers for each sugar series—including the 6-deoxyhexoses (DO), aldohexoses (AL), and hexuronic acids (UA)—will be discussed first. An in-depth evaluation of the significant changes in anomeric and conformational preference upon oxidation or reduction will follow, in addition to an evaluation of calculated Boltzmann population distributions for each isomer.

The relative gas phase free energies of the lowest energy conformers for each monosaccharide isomer are presented in Table 1, including the α- and β-anomers for both chair conformations, $^4C_1$ and $^1C_4$ (a compilation of all 3D ball-and-stick structures for all sugar series, as well as enthalpies, entropies, and ZPEs are provided in the SI, Figs. S3–S5). Free energies are calculated relative to the lowest energy structure in each sugar series, as indicated by superscript a (i.e., 6-deoxy-α-glucose, α-galactose, α-glucuronic acid). Not surprisingly, all 6-deoxyhexose and aldohexose isomers were found to favor the $^4C_1$ chair, regardless of anomeric orientation. However, several hexuronic acid isomers in the $^1C_4$ chair were found to be lower in energy than those in the $^4C_1$ chair conformation (vide infra), as will be discussed in the next section. Clearly, a picture of predominantly $^4C_1$ chair conformations does not hold when intrinsic stabilities are evaluated for all anomers of all possible glucose isomers as the C-6 oxidation state changes.

Changes in conformational preference upon oxidation or reduction at the 6-position

A comparison of the relative free energies between both chair conformers reveals that the ring conformational preference is affected for three β-isomers within the series. Oxidation to the carboxylic acid moiety resulted in a shift in equilibrium to favor the $^1C_4$ chair for β-alluronic acid, β-guluronic acid, and β-iduronic acid. It should be noted that the α-anomers of these structures favor the $^4C_1$ conformation, as well as all of the 6-deoxyhexoses and aldohexoses, as expected. The switch in conformational preference upon oxidation from the aldohexose to the hexuronic acid is illustrated in Fig. 2 for all three sugars. The ball-and-stick structures of the lowest energy rotamers for each isomer are shown, as well as the difference between the relative free energy values for $^4C_1$ and $^1C_4$ [$\Delta(\Delta G)_{FAV}$]. A negative $\Delta(\Delta G)_{FAV}$ value corresponds to favoring of the $^4C_1$ chair conformation, whereas a positive $\Delta(\Delta G)_{FAV}$ value corresponds to the $^1C_4$ conformation favored. Although all other isomers showed preference for the $^4C_1$ conformation, β-alluronic acid, β-guluronic acid, and β-iduronic acid favor the $^1C_4$ chair. It is interesting to note that all three isomers contain an axial hydroxyl group at the 3-position and equatorial hydroxyl at the 1-position (β-anomer). However, β-altruonic acid, which also has an axial 3-OH, does not follow this trend, but favors the $^4C_1$ conformation by 1.38 kcal mol^{-1}.

Previous studies on iduronic acid (IdoA) using MD simulations suggest a dynamic equilibrium between the $^4C_1$ and $^1C_4$ chairs with a small contribution of the ^2S_O conformer, where ring instability is largely attributed to C5 carboxyl epimerization [37–39]. The IdoA $^1C_4$ conformer was previously calculated to be 0.9 kcal mol^{-1} more stable than the $^4C_1$ chair, comparable to the 1.38 kcal mol^{-1} difference found within this study [40]. Neither guluronic nor alluronic acid had been modeled prior to this work, and here the $^1C_4$ conformers were found to be 0.65 kcal mol^{-1} and 0.04 kcal mol^{-1} lower in energy than their $^4C_1$ conformations, respectively. Given that these energetic differences are relatively small, it is probable that equilibrium between both chair conformations also exists for β-alluronic acid and β-guluronic acid in low dielectric media, as previously found for iduronic acid. These conformational effects related to an increase in oxidation state at C-6 have the potential to be used to direct synthetic strategies—such as use of a β-favoring mannuronic acid as a precursor β-linked mannans [60]—to improve approaches for stereoselective control in glycosylation reactions. In addition, the inherent flexibility of these three structures suggests a valuable starting point for materials development, and also for deconvoluting the structure–function relationships for biomolecules containing these monosaccharide units.

Changes in anomeric preference upon oxidation or reduction at the 6-position

A comparison of the relative free energies for each monosaccharide anomer clearly demonstrates that the preference of the α- or β-anomer can also be affected by remote oxidation or reduction at the C-6 position, and any trends depend on the identity of the specific isomer. Although the majority of isomers energetically favor the α-anomer in the gas phase regardless of conformation or oxidation state due to the anomeric effect, changes in anomeric preference are observed for derivatives of allose, idose, mannose, and talose. More specifically, both the aldohexose and hexuronic acid derivatives of allose and idose in the $^4C_1$ chair favor the α-anomer, while reduction of the 6-position to either 6-deoxy-allose or 6-deoxy-idose results in a shift of preference to

Table 1 Relative free energies (kcal mol^{-1}) of the lowest energy rotamers of the 6-deoxyhexose (DO), aldohexose (AL), and hexuronic acid (HA) sugar series in the $^4C_1$ and $^1C_4$ chair conformation at the M05-2X/cc-pVTZ(−f) level of theory (in vacuo)

6-Deoxyhexoses		Aldohexoses		Hexuronic Acids	
Isomer (Conformation)	Δ(ΔG)	Isomer (Conformation)	Δ(ΔG)	Isomer (Conformation)	Δ(ΔG)
α-dAll (4C1)	0.61	α-All (4C1)	0.19	α-AllA (4C1)	0.60
β-dAll (4C1)	0.38	β-All (4C1)	0.82	β-AllA (4C1)	3.23
α-dAll (1C4)	3.84	α-All (1C4)	4.37	α-AllA (1C4)	2.49
β-dAll (1C4)	4.05	β-All (1C4)	4.64	β-AllA (1C4)	2.58
α-dAlt (4C1)	2.11	α-Alt (4C1)	1.28	α-AltA (4C1)	0.28
β-dAlt (4C1)	2.13	β-Alt (4C1)	1.40	β-AltA (4C1)	0.95
α-dAlt (1C4)	4.44	α-Alt (1C4)	5.23	α-AltA (1C4)	3.51
β-dAlt (1C4)	3.42	β-Alt (1C4)	3.82	β-AltA (1C4)	2.33
α-dGal (4C1)	0.56	α-Gal (4C1)[a]	0.00[a]	α-GalA (4C1)	2.38
β-dGal (4C1)	1.81	β-Gal (4C1)	2.20	β-GalA (4C1)	3.30
α-dGal (1C4)	6.77	α-Gal (1C4)	7.21	α-GalA (1C4)	4.01
β-dGal (1C4)	7.39	β-Gal (1C4)	7.11	β-GalA (1C4)	3.94
α-dGlc (4C1)[a]	0.00[a]	α-Glc (4C1)	0.35	α-GlcA (4C1)[a]	0.00[a]
β-dGlc (4C1)	0.93	β-Glc (4C1)	1.28	β-GlcA (4C1)	2.24
α-dGlc (1C4)	6.18	α-Glc (1C4)	6.84	α-GlcA (1C4)	3.51
β-dGlc (1C4)	7.48	β-Glc (1C4)	7.02	β-GlcA (1C4)	4.68
α-dGul (4C1)	2.66	α-Gul (4C1)	1.63	α-GulA (4C1)	3.14
β-dGul (4C1)	1.58	β-Gul (4C1)	1.32	β-GulA (4C1)	2.51
α-dGul (1C4)	4.35	α-Gul (1C4)	5.26	α-GulA (1C4)	3.64
β-dGul (1C4)	5.27	β-Gul (1C4)	5.06	β-GulA (1C4)	2.47
α-dIdo (4C1)	3.28	α-Ido (4C1)	1.45	α-IdoA (4C1)	2.97
β-dIdo (4C1)	2.62	β-Ido (4C1)	1.49	β-IdoA (4C1)	3.71
α-dIdo (1C4)	4.16	α-Ido (1C4)	4.94	α-IdoA (1C4)	4.13
β-dIdo (1C4)	3.81	β-Ido (1C4)	3.84	β-IdoA (1C4)	2.33
α-dMan (4C1)	0.96	α-Man (4C1)	0.75	α-ManA (4C1)	0.21
β-dMan (4C1)	1.09	β-Man (4C1)	1.11	β-ManA (4C1)	0.02
α-dMan (1C4)	5.15	α-Man (1C4)	5.93	α-ManA (1C4)	3.37
β-dMan (1C4)	7.53	β-Man (1C4)	6.91	β-ManA (1C4)	4.59
α-dTal (4C1)	0.66	α-Tal (4C1)	1.05	α-TalA (4C1)	1.71
β-dTal (4C1)	1.00	β-Tal (4C1)	0.28	β-TalA (4C1)	2.05
α-dTal (1C4)	4.46	α-Tal (1C4)	5.80	α-TalA (1C4)	3.57
β-dTal (1C4)	5.98	β-Tal (1C4)	5.02	β-TalA (1C4)	4.34

[a] Lowest energy calculated structure in each of the three series

the β-anomer (Fig. 3). A change in intrinsic anomeric preference upon oxidation is also observed for mannose; mannuronic acid is shown to favor the β-anomer (0.19 kcal mol^{-1}), whereas 6-deoxy-mannose and mannose favor the α-anomer by 0.13 and 0.36 kcal mol^{-1}, respectively. A similar trend is observed for talose, where taluronic acid and talose are shown to favor the α-anomer, while 6-deoxy-talose prefers the β-anomer. All other isomers in the $^4C_1$ conformation favor only the α- or β-anomer regardless of oxidation state variation.

Regarding isomers in the $^1C_4$ chair conformation, the change in anomeric preference is now observed for derivatives of galactose, gulose and talose (Fig. 4). The aldohexose and hexuronic acid structures for galactose and gulose were found to favor the β-anomer, while their 6-deoxy-hexose derivatives favored the α-anomer. Additionally, 6-deoxy-talose and taluronic acid are observed to favor the α-anomer, while a shift in preference for the β-anomer is observed for the talose isomer. It is interesting to note that all of these structures commonly share the presence of an axial hydroxyl group at the 4-position, but that a change in anomeric preference is not observed for idose, which also has a 4-position axial hydroxyl. Idose, however, favors the β-anomer in all oxidation states.

Boltzmann population distribution and predicted anomeric ratios

The calculated percentage of each anomer in both chair conformations, as well as anomeric ratios, and conformational

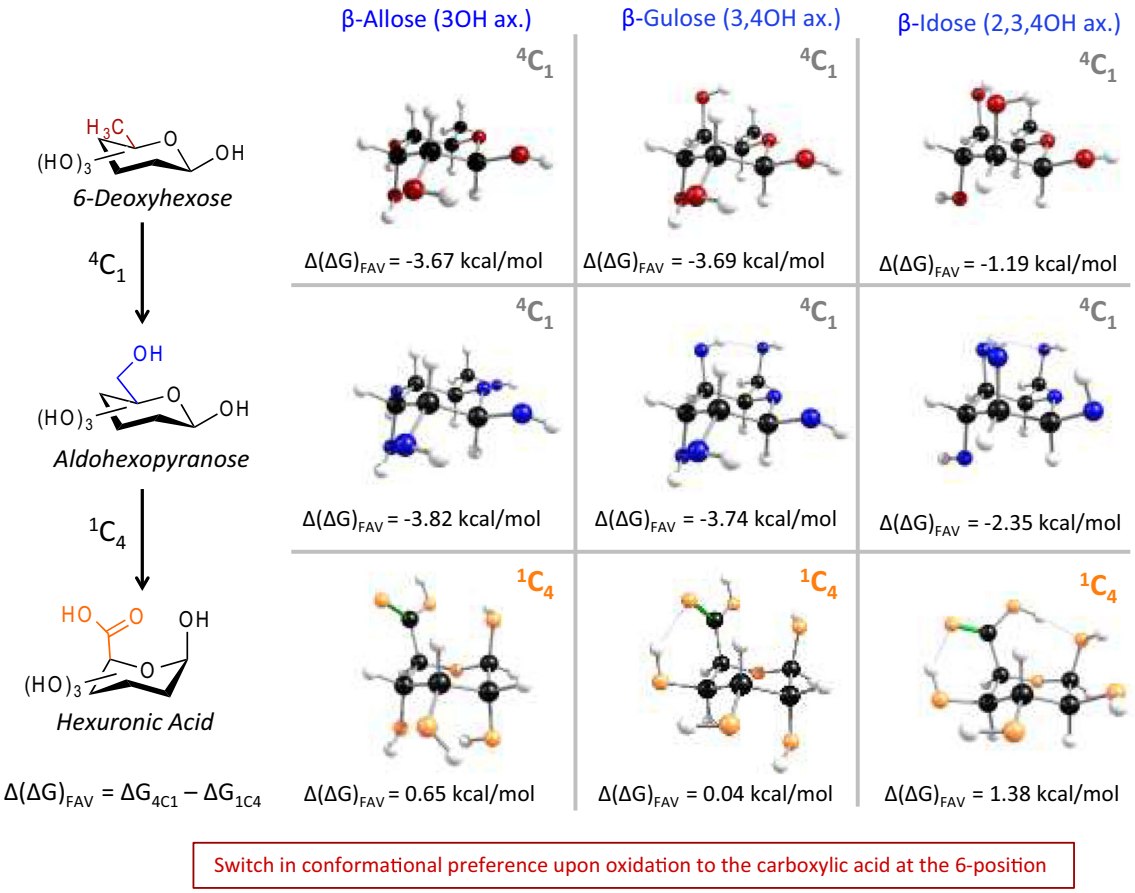

Fig. 2 Changes in ring conformational preference with varying oxidation state at C-6 (sugars not depicted favor the $^4C_1$ conformation in all oxidation states). Gibbs free energy values (kcal mol^{-1}) are calculated as the difference between the $^4C_1$ and $^1C_4$ chair conformations [$\Delta(\Delta G)_{FAV} = \Delta G_{4C1} - \Delta G_{1C4}$]

preferences are provided in Table 2 (for an expanded version, see Tables S2–S7). All values have been calculated using the Boltzmann distribution and include the total ensemble of rotamers for each given isomer.

The anomeric ratios of the aldohexose series match well to those previously reported in the literature, with the exception of idose and mannose, where the opposite anomers are favored [28]. These discrepancies can be attributed to inherent error within the calculated free energy values, and convergence to multiple other non-canonical conformers, resulting in a bias favoring the β-anomer, as reported by the authors. A comparison of the anomeric ratios between the three sugar

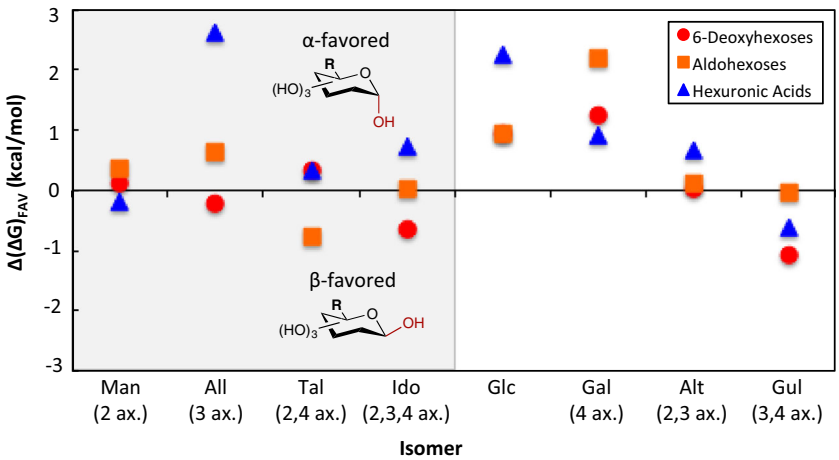

Fig. 3 Changes in $^4C_1$ ring anomeric preference with varying oxidation state at C-6 (sugars in which a change in anomeric preference occurs are highlighted in the gray box). Gibbs free energy values (kcal mol^{-1}) are calculated as the difference between the β- and α-anomer [Δ(ΔG)FAV = ΔGβ–ΔGα]

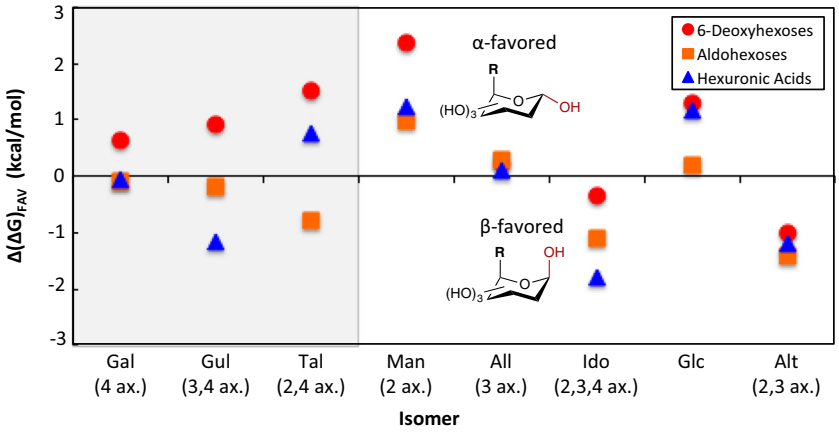

Fig. 4 Changes in $^1C_4$ ring anomeric preference with varying oxidation state at C-6 (sugars in which a change in anomeric preference occurs are highlighted in the gray box). Gibbs free energy values (kcal mol^{-1}) are calculated as the difference between the β- and α-anomer [$\Delta(\Delta G)_{FAV} = \Delta G_\beta - \Delta G_\alpha$]

series [6-deoxyhexoses (DO), aldohexoses (AL), hexuronic acids (UA)], reveals several trends associated with changes in anomeric preference in relation to varying oxidation state at C-6. Notably, the preference for the α-anomer of allose increases upon increasing the oxidation state (49:51 DO/83:17 AL/94:6 UA). A similar result was observed for glucose (84:16 DO/86:14 AL/99:1 UA) and altrose (40:60 DO/67:33 AL/73:27 UA), where a minor increase in preference for the α-anomer also results from increasing the oxidation state at C-6. The opposite trend is shown for mannose, where the β-anomer becomes slightly more favored upon reduction (63:37 DO/60:40 AL/46:54 UA). Lastly, upon reduction or oxidation at the C-6 position of idose, the β-anomer is highly favored while the α-anomer is preferred for the aldohexose structure (23:77 DO/71:29 AL/16:84 UA). No significant trends were found for the additional isomers within the series where only small changes in anomeric ratios were observed. All structures were also calculated at the B3LYP and B3LYP-D3 level of theory. A comparison of their Boltzmann distributions to the M05-2X functional can be found in the SI (Tables S2–S7), where similar results were observed with a few exceptions for select sugars, notably mannose and idose.

Table 2 Boltzmann distributions of the total ensemble of rotamers for all sugar series at the M05-2X/cc-pVTZ(−f) level of theory (in vacuo)

Monosaccharide	α:β Ratio	Preferred anomer	4C1:1C4 Ratio	Preferred conformation
6-Deoxy-allose	49:51	β	99.57:0.43	$^4C_1$
6-Deoxy-altrose	40:60	β	96.75:3.24	$^4C_1$
6-Deoxy-galactose	92:8	α	99.99:0.01	$^4C_1$
6-Deoxy-glucose	84:16	α	100:0	$^4C_1$
6-Deoxy-gulose	41:59	β	99.19:0.81	$^4C_1$
6-Deoxy-idose	23:77	β	95.3:4.7	$^4C_1$
6-Deoxy-mannose	63:37	α	99.96:0.04	$^4C_1$
6-Deoxy-talose	49:51	β	99.95:0.04	$^4C_1$
Allose	83:17	α	99.90:0.11	$^4C_1$
Altrose	67:33	α	98.84:1.16	$^4C_1$
Galactose	90:10	α	100:0	$^4C_1$
Glucose	86:14	α	99.99:0.01	$^4C_1$
Gulose	33:67	β	99.64:0.36	$^4C_1$
Idose	71:29	α	97.83:2.17	$^4C_1$
Mannose	60:40	α	99.97:0.03	$^4C_1$
Talose	39:61	β	99.97:0.03	$^4C_1$
Alluronic Acid	94:6	α	91.86:8.13	$^4C_1$
Alturonic Acid	73:27	α	96.18:3.82	$^4C_1$
Galacturonic Acid	90:10	α	93.74:6.26	$^4C_1$
Glucuronic Acid	99:1	α	99.39:0.61	$^4C_1$
Guluronic Acid	48:52	β	48.3:51.7	$^1C_4$
Iduronic Acid	16:84	β	26.78:73.22	**$^1C_4$**
Mannuronic Acid	46:54	β	99.7:0.3	$^4C_1$
Taluronic Acid	49:51	β	97.36:2.64	$^4C_1$

Conclusions

Clearly, knowledge of the 3D structure of carbohydrates is not necessarily intuitive based on knowledge of only the canonical glucose structure, and is highly dependent on exocyclic substituent stereochemistry and identity.

Oxidation or reduction of the hydroxymethyl group has been shown to have a significant influence on the inherent conformation of the pyranose ring and on anomeric stabilities. These results imply that altering the exocyclic substituents on the pyranose ring—such as with hydroxyl protecting groups—likely also has a noticeable effect on the overall shape and electronic structure of the sugar, and those changes can lead to differences in reactivity and various physical properties—a focus of future work.

One of the most interesting aspects of this comprehensive comparative computational study showed that changes in the oxidation state at the C-6 position has a considerable effect on conformational preference. Three hexuronic acid isomers including β-alluronic acid, β-guluronic acid, and β-iduronic acid were found to favor the less commonly populated $^1C_4$

conformation. Factoring in the total rotamer ensemble, interesting results were also found regarding calculated anomeric ratios. In the gas phase, the anomeric effect would be expected to dominate and favor only the α-anomer, regardless of the stereochemistry of the other substituents on the pyranose ring. However, as observed in this study and other more limited studies, several of the hexopyranose isomers were shown to favor the β-form. Specifically, oxidation to the carboxylic acid or reduction to the methyl group for allose, mannose, talose, and idose in the $^4C_1$ chair altered the anomeric preference significantly, switching preference from one anomer to the other. Those that showed a similar effect in the $^1C_4$ chair included galactose, gulose, and talose. These intriguing findings point to many future experimental possibilities to test the predictive role of such ground state structures in determining glycosylation reaction outcomes in aprotic, low dielectric media—especially those that proceed through an SN2-type mechanism.

Work is ongoing to investigate alternate modifications of the exocyclic substituents at various positions around the pyranose ring to expand our understanding of the electronic and steric factors influencing preferred conformational states. Using computational methods to quickly uncover these conformational effects can provide the carbohydrate community a more structured and focused approach to experimental design and ultimately lead to the development of synthetic rules that can be used to drive more efficient carbohydrate syntheses. Applications in the development of analytical techniques can also be envisioned, considering that the increasing use of ion mobility-mass spectrometry (IM-MS) to distinguish carbohydrate structures based on their collisional cross-sections in the gas phase requires a good understanding of the shapes of these sugars [61–63]. Knowledge of 3D carbohydrate structure can also benefit carbohydrate-based therapeutic design and the rational modification of the chemical and physical properties of drugs and materials based on sugars.

Acknowledgments This material is based in part upon work supported by the National Science Foundation under CHE-1362213. A.V. acknowledges partial support for this work as a Quantitative and Chemical Biology Training Program Fellow as part of the National Institutes of Health-supported program (1 T32 GM109825-01). This research was supported in part by Lilly Endowment, Inc. through its support for the Indiana University Pervasive Technology Institute, and in part by the Indiana METACyt Initiative. The Indiana METACyt Initiative at IU is also supported in part by Lilly Endowment, Inc. We thank the Institute for Basic Science in Korea for partial support of this work (IBS-R10-D1).

Compliance with ethical standards

Conflict of interest The authors declare no competing financial interests.

References

1. Satoh H, Manabe S (2013) Design of chemical glycosyl donors: does changing ring conformation influence selectivity/reactivity? Chem Soc Rev 42:4297–4309
2. DeMarco M, Woods R (2008) Structural glycobiology: a game of snakes and ladders. Glycobiology 18:426–440
3. National Research Council (US) Committee on Assessing the Importance and Impact of Glycomics and Glycoscience (2012) Transforming Glycoscience: a roadmap for the future. National Academies Press, Washington, DC
4. Widmalm G (2013) A perspective on the primary and three-dimensional structures of carbohydrates. Carbohydr Res 378:123–132
5. McNaught A (1996) Nomenclautre of carbohydrates. Pure Appl Chem 68:1919–2008
6. Wormald M, Petrescu A, Pao Y, Glithero A, Elliott T, Dwek R (2002) Conformational studies of oligosaccharides and glycopeptides: complementarity of NMR, X-ray crystallography, and molecular modeling. Chem Rev 102:371–386
7. Gonzalez-Outeirino J, Kirschner KN, Thobhani S, Woods RJ (2006) Reconciling solvent effects on rotamer populations in carbohydrates—a joint MD and NMR analysis. Can J Chem 84:569–579
8. Kurihara Y, Ueda K (2006) An investigation of the pyranose ring interconversion path of alpha-L-idose calculated using density functional theory. Carbohydr Res 341:2565–2574
9. Momany F, Appell M, Willett JL, Schnupf U, Bosma W (2006) DFT study of alpha- and beta-D-galactopyranose at the B3LYP/6-311++G** level of theory. Carbohydr Res 341:525–537
10. Mason PE, Neilson GW, Enderby JE, Saboungi ML, Cuello G, Brady JW (2006) Neutron diffraction and simulation studies of the exocyclic hydroxymethyl conformation of glucose. J Chem Phys 125:224505–224509
11. Suzuki T, Kawashima H, Sota T (2006) Conformational properties of and a reorientation triggered by sugar-water vibrational resonance in the hydroxymethyl group in hydrated β-glucopyranose. J Phys Chem B 110:2405–2418
12. Miura N, Taniguchi T, Monde K, Nishimura S (2006) A theoretical study of α- and β-D-glucopyranose conformations by the density functional theory. Chem Phys Lett 419:326–332
13. Schnupf U, Willett JL, Bosma W, Momany F (2007) DFT study of α- and β-D-allopyranose at the B3LYP/6-311++G** level of theory. Carbohydr Res 342:196–216
14. Biarnes X, Ardevol A, Planas A, Rovira C, Laio A, Parrinello M (2007) The conformational free energy landscape of β-D-glucopyranose Implications for substrate preactivation in β-glucoside hydrolases. J Am Chem Soc 129:10686–10693
15. Kräutler V, Müller M, Hünenberger PH (2007) Conformation, dynamics, solvation and relative stabilities of selected β-hexopyranoses in water: a molecular dynamics study with the GROMOS 45A4 force field. Carbohydr Res 342:2097–2124
16. Barnett CB, Naidoo KJ (2008) Stereoelectronic and solvation effects determine hydroxymethyl conformational preferences in monosaccharides. J Phys Chem B 112:15450–15459
17. Roslund MU, Tahtinen P, Niemitz M, Sjoholm R (2008) Complete assignments of the 1H and 13C chemical shifts and JH,H coupling constansts in NMR spectra of D-glucopyranose and all D-glucopyranosyl-D-glucopyranosides. Carbohydr Res 343:101–112
18. Suzuki T (2008) The hydration of glucose: the local configuration in sugar-water hydrogen bonds. Phys Chem Chem Phys 10:96–105
19. Guvench O, Greene S, Kamath G, Brady J, Venable R, Pastor R, Mackerell A (2008) Additive empirical force field for hexopyranose monosaccharides. J Comput Chem 29:2543–2564
20. Bosma W, Schnupf U, Willet JL, Momany F (2009) Density functional study of the infrared spectrum of glucose and glucose

monohydrates in the OH stretch region. J Mol Struct (THEOCHEM) 905:59–69
21. Spiwok V, Králová B, Tvaroška I (2010) Modelling of β-D-glucopyranose ring distortion in different force fields: a metadynamics study. Carbohydr Res 345:530–511
22. Autieri E, Sega M, Pederiva F, Guella G (2010) Puckering free energy of pyranoses: a NMR and metadynamics-umbrella sampling investigation. J Chem Phys 133:095104
23. Barnett C, Naidoo K (2010) Ring puckering: a metric for evaluating the accuracy of AM1, PM3, PM3CARB-1, and SCC-DFTB carbohydrate QM/MM simulations. J Phys Chem B 114:17142–17154
24. Mayes H, Broadbelt L, Beckham G (2014) How sugars pucker: electronic structure calculations map the kinetic landscape of five biologically paramount monosaccharides and their implications for enzymatic catalysis. J Am Chem Soc 136:1008–1022
25. Silla J, Cormanich R, Rittner R, Freitas M (2014) Does intramolecular hydrogen bond play a key role in the stereochemistry of α- and β-D-glucose? Carbohydr Res 396:9–13
26. Plazinski W, Drach M (2015) Kinetic characteristics of conformational changes in the hexopyranose rings. Carbohydr Res 416:41–50
27. Uddin N, Ghosh M, Choi T, Choi C (2015) Gauche effects of glucopyranose by QM/MM-MD simulations. Theor Chem Accounts 134:122
28. Schnupf U, Willett JL, Momany FA (2010) DFTMD studies of glucose and epimers: anomeric ratios, rotamer populations, and hydration energies. Carbohydr Res 345:503
29. Appell M, Strati G, Willett JL, Momany FA (2004) B3LYP/6-311++G** study of α- and β-D-glucopyranose and 1,5-anhydro-D-glucitol: 4C1 and 1C4 chairs, 3,OB and B3,O boats, and skew. Carbohydr Res 339:537–551
30. Barrows S, Storer J, Cramer C, French A, Truhlar DG (1998) Factors controlling relative stability of anomers and hydroxymethyl conformers of glucopyranose. J Comput Chem 19:1111–1129
31. Polavarapu P, Ewig C (1992) Ab initio computed molecular structures and energies of the conformers of glucose. J Comput Chem 13:1255–1261
32. Patel D, He X, MacKerell A (2015) Polarizable empirical force field for hexopyranose monosaccharides based on the classical drude oscillator. J Phys Chem 119:637–652
33. Csonka G, Éliás K, Csizmadia I (1996) Ab initio and density functional study of the conformational space of 1C4 α-L-fucose. J Comput Chem 18:330–342
34. Csonka G, Éliás K, Kolossváry I, Sosa C, Csizmadia I (1998) Theoretical study of alternative ring forms of α-L-fucopyranose J Phys Chem A 102:1219–1229
35. Nyerges B, Kovács A (2005) Density functional study of the conformational space of 4C1 D-glucuronic acid. J Phys Chem A 109: 892–897
36. Remko M, von der Lieth C (2006) Gas-phase and solution conformations of the α-L-iduronic acid structural unit of heparin. J Chem Inf Model 46:1194–1200
37. Sattelle B, Hansen S, Gardiner J, Almond A (2010) Free energy landscapes of iduronic acid and related monosaccharides. J Am Chem Soc 132:13132–13134
38. Ochsenbein P, Bonin M, Schenk-Job K, El-Hajji M (2011) The 2SO skew-boat conformation in L-iduronic acid. Angew Chem Int Ed 50:11637–11639
39. Oborský P, Tvaroška I, Králová B, Spiwok V (2013) Toward an accurate conformational modeling of iduronic acid. J Phys Chem B 117:1003–1009
40. Klepach T, Zhao H, Hu X, Zhang W, Stenutz R, Hadad MJ, Carmichael I, Serianni AS (2015) Informing saccharide structural NMR studies with density functional theory calculations. Methods Mol Biol 1273:289–331
41. Turney T, Pan Q, Sernau L, Carmichael I, Wenhui Z, Xiaocong W, Woods R, Serianni AS (2016) O-acetyl side-chains in monosaccharides: redundant NMR spin-couplings and statistical models for acetate ester conformational analysis. J Phys Chem B 121:66–67
42. Cramer C (1992) Anomeric and reverse anomeric effects in the gas phase and aqueous solution. J Org Chem 57:7034
43. Molteni C, Parrinello M (1998) Glucose in aqueous solution by first principles molecular dynamics. J Am Chem Soc 120:2168
44. Brady J (1989) Molecular-dynamics simulations of alpha-D-glucose in aqueous solution. J Am Chem Soc 111:5155
45. Momany FA, Schnupf U (2014) DFT optimization and DFT-MD studies of glucose, ten explicit water molecules enclosed by an implicit solvent, COSMO. Comput Theor Chem 1029:57–67
46. Tomasi J, Mennucci B, Cammi R (2005) Quantum mechanical continuum solvation models. Chem Rev 105:2999–3093
47. Serena Software Box Bloomington, IN 47402–3076. http://www.serenasoft.com
48. Gajewski J, Gilbert K, McKelvey J (1990) MMX molecular mechanics calculations (enhanced MM2 variant). Adv Mol Mod 2:65–92
49. Burket U, Allinger N (1982) Molecular Mechanics. ACS Monograph 177. American Chemical Society, Washington, DC
50. Allinger N, Yuh Y (1982) MM2 Program, QCPE 395. Quantum Chemistry Program Exchange, Indiana
51. Jaguar version 7.7 (2010) Schrodinger, LLC, New York, NY
52. Becke A (1989) Density-functional thermochemistry. III. The role of exact exchange. J Chem Phys 98:5648–5652
53. Zhao Y, Schultz NE, Truhlar DG (2006) Design of density functionals by combining the method of constraint satisfaction with parameterization for thermochemistry, thermochemical kinetics, and noncovalent interactions. J Chem Theory Comput 2:364–382
54. Dunning T (1989) Gaussian basis sets for use in correlated molecular calculations. I. The atoms boron through neon and hydrogen. J Chem Phys 90:1007–1023
55. Sameera WMC, Pantazis D (2012) A hierarchy of methods for the energetically accurate modeling of isomerism in monosaccharides. J Chem Theory Comput 8:2630–2645
56. Csonka G, French A, Johnson G, Stortz C (2009) Evaluation of density functionals and basis sets for carbohydrates. J Chem Theory Comput 5:679–692
57. Zhao Y, Truhlar D (2008a) Density functionals with broad applicability in chemistry. Acc Chem Res 41:157–167
58. Zhao Y, Truhlar D (2006) Assessment of model chemistries for noncovalent interactions. J Chem Theory Comput 2:1009–1018
59. Zhao Y, Truhlar D (2008b) The M06 suite of density functionals for main group thermochemistry, thermochemical kinetics, noncovalent interactions, excited states, and transition elements: two new functionals and systematic testing of four M06-class functionals and 12 other functionals. Theor Chem Account 120:215–241
60. Tang SL, Pohl NLB (2015) Automated solution phase synthesis of β-1,4-mannuronate and β-1,4-mannan. Org Lett 17:2642–2645
61. Gaye M, Nagy G, Clemmer DE, Pohl NLB (2016) Multidimensional analysis of 16 glucose isomers by ion mobility spectrometry. Anal Chem 88:2335–2344
62. Both P et al (2014) Discrimination of epimeric glycans and glycopeptides using IM-MS and its potential for carbohydrate screening. Nat Chem 6:65–74
63. Hofmann J, Hahm HS, Seeberger PH, Pagel K (2015) Identification of carbohydrate anomers using ion mobility-mass spectrometry. Nature 526:241–244